# The cytotoxicity of Epsilon toxin from *Clostridium perfringens* on lymphocytes is mediated by MAL protein expression

Running title: Effect of epsilon toxin on T-cells

Marta Blanch [a,b,c], Jonatan Dorca-Arévalo [a,b,c], Anna Not [a], Mercè Cases [a,b,c], Inmaculada Gómez de Aranda [a,c], Antonio Martínez Yélamos [b,d], Sergio Martínez Yélamos [b,d], Carles Solsona [a,b,c] and Juan Blasi [a,b,c#]

[a] Laboratory of Cellular and Molecular Neurobiology, Department of Pathology and Experimental Therapeutics, Campus of Bellvitge, University of Barcelona, Hospitalet de Llobregat, Barcelona, Spain,

[b] Biomedical Research Institute of Bellvitge (IDIBELL), Hospitalet de Llobregat, Barcelona, Spain,

[c] Institute of Neurosciences, University of Barcelona, Barcelona 08035, Spain,

[d] Neurology Department. Bellvitge University Hospital. Hospitalet de Llobregat, Barcelona, Spain,

# Address correspondence to Juan Blasi, blasi@ub.edu

Word count: 10113

Material and Methods: 3416

Introduction, Results and Discussion: 3464

## ABSTRACT

Epsilon toxin (Etx) from *Clostridium perfringens* is a pore-forming protein that crosses the Blood-Brain Barrier, binds to myelin and hence, has been suggested as a putative agent for the onset of multiple sclerosis, a demyelinating neuroinflammatory disease. Recently, Myelin and Lymphocyte protein (MAL) has been identified as a key protein in the cytotoxic effect of Etx, however the association of Etx with the immune system remains a central question. Here, we show that Etx selectively recognizes and kills only human cell lines expressing MAL through a direct Etx-MAL interaction. Experiments on lymphocytic cell lines reveal that MAL expressing T cells, but not B cells, are sensitive to Etx, and revealed the toxin as a molecular tool to distinguishing subpopulations of lymphocytes. The overall results open the door to investigate the role of Etx and *Clostridium perfringens* on inflammatory and autoimmune diseases like multiple sclerosis.

Molecular and Cellular Biology

## INTRODUCTION

Epsilon toxin (Etx) from *Clostridium perfringens* toxinotypes B and D is the most powerful toxin after botulinum and tetanus toxins, mainly affecting ruminants causing important economic losses (1). The toxin is produced by the bacteria present in the guts of young animals leading to fatal enterotoxemia in sheep, goat and cattle (2, 3). It is synthesized as a non-toxic protein precursor, epsilon-prototoxin (pEtx), which is activated upon proteolytic cleavage at the N and C-terminal regions (4).

In addition to its effect on livestock, Etx has a lethal activity when injected into experimental animal models, basically, rodents. Etx bypasses the transit through the digestive system and causes a generalized edema, neurological disorders and, finally, the death of the animal, being the lethal dose in mice (one of the most used animal model for Etx studies) around 100 ng/Kg (5). At the cellular level, Etx is a member of the aerolysin-like ß-pore forming toxin family (6). Etx form pores in lipid planar bilayers and therefore in the plasma membrane of sensitive cells after its specific binding and further oligomerization, producing cell permeability, ionic diffusion, ATP depletion and cell death (7, 8). The toxin also has the capacity to cross the Blood-Brain Barrier (BBB) and bind to cerebral myelin (9, 10). Moreover, “in vitro” experiments using primary cell cultures and brain explants, demonstrate the demyelination capacity of Etx and eventually a cytotoxic effect on oligodendrocytes (10, 11), the myelin forming cells in the central nervous system. These and other evidences have been used as arguments to suggest Etx as a putative agent for the onset of multiple sclerosis, a neuroinflammatory disease with a demyelinating component (12).

In addition to the effect of Etx on oligodendrocytes, few cell lines have been defined to be sensitive to Etx and identified as potential targets of its cytotoxic activity. Among them, the most sensitive cell line is MDCK (Madin-Darby Canine Kidney), a renal epithelial distal tubule cell line from canine origin, which has been widely used to study the cellular and molecular mechanism of Etx cytotoxicity (8). This characteristic of the renal cell line correlates with the observed "in vivo" cytotoxic effect of Etx on renal distal tubular cells in Etx injected mice (13, 14). Other cell lines sensitive to Etx but with a variable cytotoxic effect depending on the cell model include the mouse kidney cell line mpkCCD$_{c14}$ (15), the Caucasian renal leiomyoblastoma (G-402) human cell line (16), primary cultures of human renal tubular epithelial cells (HRTEC) (17) and the human renal adenocarcinoma cell line ACHN (18) among others.

It is assumed that the specific action of Etx on sensitive cells relies on the presence of an Etx receptor to selectively bind the cell surface before the formation of the oligomer. In spite of the proposed role of membrane lipids in the recognition or affinity of Etx to the cell targets (19-21), a set of proteins has been explored as potential receptors for Etx, which can account for the full and high sensitive effect of the toxin. Among them, the most promising candidates are the hepatitis A virus cellular receptor 1 (HAVCR1) (18), and the Myelin and Lymphocyte protein (MAL) (22). While a complete functional evidence for HAVCR1 as an Etx receptor mediating its cytotoxic activity is elusive (23), the transfection of MAL protein confers sensitivity to otherwise unresponsive cell lines (22). In addition, KO mice for MAL protein survive after intraperitoneal injection of a lethal dose of Etx (22). Accordingly, Myelin and Lymphocyte

protein (MAL) has been defined as a key protein in the cytotoxic effect of Etx, either as a putative receptor or as an effector protein (23).

MAL is a tetraspanning membrane protein of 17 kDa initially identified as a marker of human T cell maturation (24). This protein is also present in myelinating oligodendrocytes, myelin and in some epithelial cells (i.e., urothelial and renal tubules) where it has been involved in membrane traffic, especially for apical transport of membrane and secretory proteins and lipid raft cycling (25, 26). The presence of MAL protein in myelin structures and myelinating oligodendrocytes would explain the specific binding of Etx to myelin (9) and the demyelinating effect of the toxin (10, 11). The presence of MAL protein in lymphocytes has been mainly linked to the maturation of T-cells (24), intracellular membrane traffic (27) or the exosome secretion (28). However, the possible effect of Etx on MAL expressing lymphocyte derived cells is not known.

In the present paper, we further explore by several methods whether the cytotoxic ability of Etx from *Clostridium perfringens* is exclusively dependent on the expression of MAL protein. Moreover, evidence of a direct interaction of MAL protein with Etx is provided by means of immunoprecipitation assays. These results led us explore the sensitivity of cell lines from lymphocytic origin to Etx, which naturally express or not MAL protein, and demonstrate that this protein is sufficient for Etx cytotoxic activity. The study of cell types that naturally express MAL protein would give a new light on the Etx action mechanism and its relationship with immune system related disorders.



Molecular and Cellular Biology

## RESULTS

### MAL is required for Etx Binding

To characterize the MAL-dependent cytotoxic effect of Etx, three cell lines which do not express MAL protein (tsA201, RT4-D6P2T and HeLa) were stably transfected, for the expression of human MAL protein (hMAL) fused to Green Fluorescent Protein (GFP), hMAL-GFP. Mock transfected cells (GFP) were used as controls.

Transfected cells were positively selected with 0.5 mg/mL Geneticin/ G418 before cell sorting was performed and the most positive cells expressing hMAL-GFP were collected, maintained and used for further experiments. The effectiveness of hMAL-GFP expression was monitored by western blot analysis using anti-GFP and anti-MAL-E1 antibodies (Figures 1A and 1B, respectively).

Confocal microscopy images revealed the expression of hMAL-GFP protein mostly localized in the cell plasma membrane, while GFP was localized in the cytosol and nuclei in mock transfected cells (Figure 1C).

Etx labelled with DyLight 633 (Etx-633) was used to verify the binding of Etx to positive hMAL-GFP expressing cells. As expected, the toxin was bound to the cell lines expressing hMAL-GFP but not to the GFP control cell lines. Most of the Etx labeling was localized in the periphery of the cells, matching the distribution of hMAL-GFP (Figure 1C).

### Etx produces cytotoxicity in hMAL expressing cells

The cytotoxic effect of Etx is based on the selective binding to the target cell, the oligomerization of the protein and the subsequent pore formation that

permeabilizes the cell plasma membrane allowing the diffusion of ions and other elements up to 2.3 kDa (29, 30).

Taking advantage of the pore forming capacity of Etx, the release of ATP from cytosol or internal cell stores was measured using the luciferine-luciferase method on hMAL-GFP expressing cells, on MDCK cells used as positive controls and on GFP transfected cells used as negative controls.

ATP release from MDCK cells was Etx dose and time dependent (Fig.2A). All content of ATP was released between 30 min (100 nM Etx) and 40 min (12.5 nM) depending on the Etx dose.

The concentrations of Etx used (from 12.5 to 100 nM) were rather high, considering the sensitivity of MDCK cell line to Etx, but this approach was very convenient because it allowed the measurement in real time of Etx-dependent ATP release in a limited time. At the end of the experiment, all ATP was virtually released by Etx and no residual ATP could be measured after cell permeabilization with Triton X-100. However, Triton X-100 released all ATP content in the case of GFP expressing cells or when pEtx was used instead of fully active Etx. These results suggest that at all concentrations used, the MDCK cells were already dead at the end of the experiment in spite of the Etx concentration used (Figure 2A).

As expected, hMAL-GFP transfected cells released ATP in the presence of Etx (Figure 2B) however no ATP was released from GFP transfected cells or from those cells incubated in the presence of pEtx, even at the highest concentration used. These results support the pore formation by Etx (anionic or non-specific) in hMAL expressing cells, although the rupture of the plasma membrane by other mechanism (i.e. necrosis) cannot be discarded.

176 The MTS ((3-(4,5-dimethylthiazol-2-yl)-5-(3-carboxymethoxyphenyl)-2-(4-
177 sulfophenyl)-2H-tetrazolium) colorimetric assay was used in cytotoxicity assays
178 to determine cell viability (see material and methods). The MTS assays
179 revealed that Etx and Etx-633 showed a similar degree of cytotoxicity on hMAL-
180 GFP expressing cells, with no effect on GFP control cells. The non-active forms
181 of the toxin, pEtx or pEtx-633 showed no toxic effects (not shown). The
182 cytotoxic effect of Etx on hMAL-GFP transfected cell lines was similar to that
183 observed in MDCK cells (Figure 3), although this effect was not complete in all
184 transfected cell lines (no 100% of cell death), suggesting different levels of
185 hMAL-GFP expression compared with the well stablished and sensitive MDCK
186 cell line. The cytotoxicity of Etx on hMAL-GFP transfected cell lines was dose
187 dependent with a maximum effect around 25 nM. The $CT_{50}$ was calculated with
188 a 95% confidence interval indicated as 95% CI (lower-upper). In the case of
189 tsA201-hMALGFP $CT_{50}$ was 1.26 nM (0.69-2.27), in RT4-D6P2T-hMALGFP
190 $CT_{50}$ was 2.88 nM (2.36-3.50) and finally in HeLa-hMALGFP $CT_{50}$ was 3.36 nM
191 (2.63-4.29). All of them were values not far from the $CT_{50}$ calculated for MDCK
192 cells, 0.64 nM (0.52-0.78).
193
194 **Direct interaction hMAL-Etx**
195 Considering that transfection of hMAL-GFP in a non-sensitive cell line is able to
196 transform this cells into Etx sensitive (as seen in MTS assays and ATP release
197 experiments), it was essential to search for a possible Etx-MAL interaction.
198 In order to check a possible Etx-MAL interaction, coimmunoprecipitation (Co-IP)
199 assays were performed with the expressing hMAL HeLa stable cell line (HeLa
200 hMAL-GFP). Four confluent culture dishes of 10 cm diameter were grown; two

of them were exposed for 30 min to 100 mM Etx, one was exposed for 30 min to 100 mM pEtx and the last one was kept as a negative control. From all dishes, total cell extracts were obtained, inputs were kept and the rest of cell lysates were incubated with anti-GFP antibody to immunoprecipitate (IP) hMAL-GFP, except in one of the extracts treated with Etx that was incubated with anti-αTubulin as a negative IP control. Western blot analysis performed after immunoprecipitation using anti-pEtx antibody, revealed that Etx coimmunoprecipitate with hMAL-GFP (Figure 4). It is remarkable that Etx is detected in inputs and in coimmunoprecipitates as a large membrane complex. It is well known that Etx oligomerizes and forms a large membrane complex, as previously described in MDCK cell line (20). Etx was not detected when using the negative control antibody (anti-αTubulin). The same membrane was subsequently incubated with anti-GFP in order to check the correct immunoprecipitation of hMAL-GFP. Thus, the coimmunoprecipitation experiments indicated that Etx and MAL are able to interact.

The above and previous results from other labs (22), suggest that MAL protein is required for the cytotoxic activity of Etx. If this is the case, those cells expressing MAL could be potential targets of Etx. This suggestion is especially relevant for those cells of the immune system that may be involved directly or indirectly with neuroinflammatory and autoimmune diseases. To further study this possibility, we took advantage of cell lines of lymphocytic origin that express MAL, and compared the results with cell lines of lymphocytic origin that do not express MAL.

**MAL protein in Lymphocytes**

MAL protein was firstly identified in subsets of human lymphocyte populations, basically T derived cell lines, as the Jurkat and MOLT-4 human lymphocyte cell lines (24). Taking advantage of the naturally expression of MAL protein in these cell lines, the possible effect of Etx was studied and compared with lymphocytic cell lines that do not express MAL protein (TK6 and JeKo-1, mantle derived cell lines). The expression of MAL mRNA in MOLT-4 and Jurkat, but not in TK6 and JeKo-1 cell lines, was corroborated by RT-PCR (Figure 5A). Notice that the 18S rRNA, used as an internal control, indicate a constant expression level across all samples.

The effect of Etx on lymphocytic cell lines expressing MAL protein was confirmed by the MTS cytotoxic assay (Figure 5B), the ATP release assay (Figure 5C) and flow cytometry (Figures 6A and 6B). All experimental approaches showed specific effect of Etx on Jurkat and MOLT-4 cell line, but not in TK6 and JeKo-1 cell lines, with a higher cytotoxic effect and ATP release on the MOLT-4 cell line. Compared to the effect of Etx on MDCK cell line with a $CT_{50}$ of 0.64 nM (0.52-0.78) the lymphocytic Etx-sensitive cell lines were slightly less sensitive. In MOLT-4 cells, the $CT_{50}$ was 11.09 nM (7.26-16.67) and in Jurkat cells the $CT_{50}$ was 26.67 nM (19.04-37.4).

Taking into account the sensitivity of lymphocytic MAL expressing cell lines to Etx, the possible formation of Etx oligomers, as a previous step for the pore formation, was analyzed. A western blot analysis was performed on MOLT-4 and JeKo-1 cells after 30 min of 100 nM pEtx and Etx incubation (Figure 6C). Western blot analysis revealed the Etx oligomeric complex formation on MOLT-4 cells but not on JeKo-1 cells nor on cells incubated with pEtx, indicating

therefore that the effect of Etx on MAL-expressing lymphocytic cell lines depends on the formation of Etx complex in the cell plasma membrane.

To fully demonstrate that the expression of MAL was a condition for Etx cytotoxic effect, the MOLT-4 cell line was used to deplete the expression of the protein by the CRISPR-Cas9 method. Several clones were obtained and analyzed for the effect of Etx, either in MAL depleted clones (MOLT-4-ΔMAL) or mock transfected (MOLT-4 CTL). The absence of MAL protein in the MOLT-4-ΔMAL clone was checked by western blot assay (Figure 7A) and the subsequent absence of Etx binding, by confocal microscopy and flow cytometry assay (Figures 7B and 7C). These experiments clearly demonstrated that the absence of MAL, directly affect Etx binding to the plasma cell membrane.

Cytotoxic assay and Etx-dependent ATP release experiments on MOLT-4-ΔMAL and MOLT-4-CTL clones, also showed the absence of Etx cytotoxic effect when MAL protein was not expressed (Figure 8A). Moreover, the absence of membrane complex formation after incubation with Etx, was also evident in MOLT-4-ΔMAL cells analyzed by western blot and compared to MOLT-4-CTL cells (Figure 8B).

## DISCUSSION

In this report, we show the direct interaction of epsilon toxin (Etx) from *Clostridium perfringens* with cells of the immune system. In humans, Etx has been involved with the onset of the neuroinflammatory and demyelinating disease, multiple sclerosis (MS) (12). As far as we know, no relationship of Etx

274 with the immune system and the possible involvement of this direct interaction
275 with neuroinflammatory disease have been described before.
276 Etx crosses the BBB and produces neurological alterations in sheep, goat,
277 cattle, mice and rats (31-33). Moreover, Etx induces glutamate release (5, 34)
278 either by membrane pore formation (8) or through a membrane transporter (10)
279 or both systems, raising intracellular receptor-mediated calcium concentration
280 and producing a cytotoxic effect (5, 8, 10, 35). In fact, lethal activity of Etx has
281 been directly related to the neurological effect (31, 36).
282 It is assumed that the Etx-dependent ATP release is mediated by the pore
283 formation of Etx, after toxin oligomerization, that allows the efflux of molecules
284 up to ~ 2300 Da from the cytosolic compartment (30). Similarly, Etx-dependent
285 glutamate efflux from cells in the CNS has been observed, although the rise in
286 extracellular glutamate has been also ascribed to glutamate membrane
287 transporter without a concomitant cytotoxic effect (10). Accordingly, ATP could
288 be, at least, partially extruded by another mechanism than through a pore
289 formation, including membrane transporters or even by necrotic cell death
290 shown in several pore forming toxins (37). In any case, extracellular ATP may
291 trigger the excitotoxicity of oligodendrocytes by the activation of P2X7
292 receptors, together with glutamate-mediated excitotoxicity (10, 38).
293
294 The present report supports a direct role of MAL protein in Etx activity (22). The
295 expression of hMAL protein in tsA201, RT4 and HeLa cell lines, that naturally
296 do not express MAL protein, is sufficient to sensitize them to Etx and,
297 accordingly, cells naturally expressing MAL protein are sensitive to Etx. The
298 effect of Etx on MAL protein expressing cells was confirmed using up to three

299 different methods: the MTS based cell cytotoxic assay and the ATP release on
300 transfected cell lines, together with the flow cytometry assay when lymphocytic
301 derived cell lines were used in the study. All three methods demonstrated the
302 cytotoxic effect of Etx in the nanomolar range only in MAL expressing cells,
303 supporting this membrane protein as the cellular Etx receptor. Interestingly,
304 MAL protein has been related to a defined membrane lipid composition,
305 basically, in glycosphingolipids enriched domains, mainly galactosilceramide
306 and sulfatide (39). Removal of the sulfate group significantly impairs Etx
307 cytotoxic activity in MDCK cells, suggesting a close relationship between MAL
308 protein, sulfatide and Etx (19). Moreover, MAL protein has been involved in
309 myelin biogenesis, probably in the vesicular transport of sulfatide to the
310 membrane forming myelin (39, 40).
311 Genetically deficient MAL mice are resistant to Etx, suggesting that MAL is not
312 only involved in the cytotoxic effect of Etx on defined target cells but also in its
313 lethal effect on naturally infected and experimental animal models.
314 As far as we know, this is the first time showing a direct effect of Etx on
315 lymphocytic cell lineage, and in particular on T cell derived lymphocytes.
316 Moreover, the cytotoxic effect of Etx coincides with the expression of MAL
317 protein in the sensitive cell lines (24) and this report, being specific and
318 dependent of MAL protein expression: MAL protein deletion in MOLT-4 cell line
319 completely abolishes the cytotoxic effect of Etx.
320 Which could be the consequence of Etx acting on immune T cells? Although it
321 is still speculative, it could represent the connection between Etx and its
322 proposed role as an agent in the onset of MS. Different possibilities can be
323 considered: a) it may represent a situation where a direct but chronic exposure

to low Etx concentrations and the property of Etx to both bind myelin and lymphocytes may induce alteration in myelin structure, in its formation or maintenance; b) Etx could have a direct effect on oligodendrocytes, producing its malfunctioning, and even degeneration, with a consequent demyelination (10, 11) or a neuroinflammatory effect that would cause also alterations in myelin structures and subsequent demyelination; c) Etx may directly act on a defined T cell population, either producing a cytotoxic effect or activating an immune response.

In the first possibility, the effect of Etx on lymphocytes would be time and concentration dependent. It could be assumed that circulating blood cells, in particular a subpopulation of T cells wearing MAL protein, would be the first cell type in contact with Etx, together with endothelial cells, once in the blood stream after toxin enters the organism even at very low amounts. Although the effect on immune cells could not be evident at such low dose and no symptoms would be visible in a short time (which could be evident when a high number of T-cell would be affected), T-cells expressing MAL could be in contact with Etx for a long time, acting as Etx carriers and eventually entering the CNS were they can interact with cells that, in turn, express MAL protein (oligodendrocytes). In the second possibility, as stated before, Etx binds to and eventually affects endothelial cells, crosses the BBB and binds to myelin (9, 41) where it may act directly on oligodendrocytes producing demyelination (10, 11). In the third possibility, Etx would act through MAL expressing T cell direct interaction. In that case, Etx could activate a defined pool of T cells (those expressing MAL) and potentiate any of the above proposed mechanism in the onset of CNS

demyelinization, or produce a cytotoxic effect on a regulatory T cell population, increasing the probability of autoimmune reaction.

We understand that these suggestions are highly speculative, but they open a new view on the onset of neuroinflammatory diseases, where particular gut microbiota component directly or indirectly interact with the immune and nervous systems, affecting particular cell functions. While Etx may be the agent responsible for a demyelinating process, other components of the microbiota may influence or precipitate its onset (42). The animal model for MS, the experimental autoimmune encephalomyelitis (EAE) is characterized by the contribution of CD4 T lymphocytes, specially Th1 and Th17 producing interferon-gamma and interleukin 17 respectively (43, 44). It is widely accepted that MS, an autoimmune disease, is triggered by autoreactive T cells, that would be antigen activated, cross the BBB and initiate an inflammatory response (45).

All together, these results show a direct interaction of Etx from *Clostridium perfringens* with T cells expressing MAL suggesting a possible role in neuroinflamatory events and point out Etx (and pEtx) as a new marker for lymphocyte T cells lineage.

## MATERIALS AND METHODS

### Cell lines

MDCK (CCL-34, ATCC): Madin-Darby canine kidney (MDCK) was used as a positive control, as is the most common sensitive *in vitro* model for Etx.

372 Three cell lines from different origin: tsA201(96121229, ECACC) from human
373 kidney, RT4-D6P2T (CRL-2768, ATCC) from a rat schwannoma and HeLa
374 (CCL-2, ATCC) a human epithelial cervix cell line from an adenocarcinoma,
375 were selected because they do not express MAL protein and are insensitive to
376 Etx.
377 Cell lines from different lymphocyte origin were chosen because of their
378 capacity to express or not MAL protein. TK6 (CRL-8015, ATCC) a human B
379 lymphoblast cell line and JeKo-1 (CRL-3006, ATCC) a mantle cell lymphoma
380 cell line, do not express MAL protein. On the other hand, Jurkat (88042803,
381 ECACC) a human leukaemic T cell lymphoblast cell line and MOLT-4
382 (85011413, ECACC) a human acute T lymphoblastic leukemia cell line, both
383 express MAL protein.
384
385 MDCK (CCL-34, ATCC), tsA201(96121229, ECACC), RT4-D6P2T (CRL-2768,
386 ATCC) and HeLa (CCL-2, ATCC) cell lines were maintained in DMEM-F12
387 medium containing 15 mM Hepes and 2.5 mM L-Glutamine (Gibco),
388 supplemented with 10% heat-inactivated fetal bovine serum (FBS) (Biological
389 Industries) and 1% Penicillin/Streptomycin (P/S) (Sigma-Aldrich).
390 TK6 (CRL-8015, ATCC), Jurkat (88042803, ECACC), MOLT-4 (85011413,
391 ECACC) and JeKo-1 (CRL-3006, ATCC) cells were maintained in RPMI
392 medium (Gibco), supplemented with 10% (FBS) (Biological industries).
393 Cells were all grown at 37ºC in a humidified atmosphere of 5% $CO_2$.
394 Cell lines including tsA201, RT4-D6P2T, HeLa, were used to obtain stably
395 transfected cells for the expression of pEGFPN1-hMAL, or pEGFPN1 as a
396 negative control. Cells were transfected using Lipofectamine 2000 (Invitrogen).

After transfection, cells were selected with 0.5 mg/mL Geneticin/G-418 (Gibco). Homogenous GFP expressing cells were obtained using the cell sorter MoFlo Astrios (Beckman Coulter) at CCiTUB, Biology Unit of the Bellvitge Campus, University of Barcelona.

**Expression of cDNA constructs of pEtx and GFP-pEtx**

Expression vectors to produce a recombinant protein with a 6 Histidine tag at the pEtx or GFP-pEtx C terminal were generated based on previously described plasmids (41). Plasmids were transformed into a RossetaTM(DE3)pLysS Escherichia coli strain for optimum protein expression. The expression of pEtx or GFP-pEtx recombinant protein was induced overnight at room temperature in 250-ml LB medium cultures containing 1mM isopropyl-ß-D-thiogalactopyranoside. Cells were pelleted and resuspended in ice cold phosphate buffer (PB) 0.01M $NaH_2PO_4$, 0.01M $Na_2HPO_4$ pH 7.4, containing 250 mM NaCl, sonicated and centrifuged at 15,000 g for 20 min at 4°C. The resulting supernatant was incubated with 0.5 ml of previously equilibrated TALON® Metal Affinity Resin previously washed with PB and eluted with PB containing 250 mM imidazole. The eluate was dialyzed with Phosphate Buffered Saline (PBS) 0.01 M phosphate buffer, 0.150 mM NaCl and 2,7 mM KCl at final pH 7.4, to eliminate imidazole and final protein content was quantified, analyzed by SDS-PAGE and stored at -20°C, until used. Full active toxin was obtained by trypsin proteolysis of pEtx or GFP-pEtx, using trypsin beads (Sigma-Aldrich), according to the manufacturer's instructions. The toxicity of pEtx and GFP-pEtx and their respective activated toxins were tested in MDCK cells as described

421 elsewhere (14). The process of purification was performed following the
422 guidelines of biosecurity of the University of Barcelona.
423
424 **Cloning pEGFPN1-hMAL**
425 hMAL coding sequence (CDS) was obtained by Polymerase chain reaction
426 (PCR) using 2 µL of a human cDNA brain library as template, 25 µL KOD Hot
427 Start DNA Polymerase (Merck Millipore), 1,5 µL oligonucleotides at 10 µM, in a
428 final 50 µL reaction volume. The oligonucleotides used were:
429 Forward, 5'-GCGAGATCTATGGCCCCCGCAGCGGCGACGGGGGG-3'
430 (containing BglII target) and
431 Reverse,5'-
432 GCGGTCGACTGTGAAGACTTCCATCTGATTAAAGAGAACACCGC-3'
433 (containing SalI target).
434 The reaction was carried out using the following parameters: 95ºC for 2 min, 40
435 cycles of 95ºC 20 s, 60ºC 10 s and 70ºC for 10 s. hMAL PCR was purified using
436 QIAquick® Gel Extraction Kit (Qiagen). Purified PCR was digested with BglII-
437 SalI restriction enzymes (Thermo Scientific) and the same enzymes were used
438 to clone hMAL into pEGFPN1. Finally, pEGFPN1-hMAL construct was
439 sequenced to confirm DNA sequence and to check DNA insert orientation.
440
441 **MAL protein detection by western blot analysis**
442 MAL protein expression in hMAL-GFP stably transfected cell lines was detected
443 by western blot analysis. Confluent 10 cm diameter culture plates were washed
444 twice with Phosphate Buffered Saline (PBS). Cells were scraped with a cell
445 scrapper (TPP) maintaining the cell plate on ice and adding 500 µL of RIPA

446 buffer (25 mM Tris-HCl pH 7.4 , 150 mM NaCl, 1% NP40, 10% SDS, 1%
447 sodium deoxycholate) supplemented with 1:100 Protease inhibitor cocktail
448 (#P8340, Sigma-Aldrich). Scrapped cells were set into a 1.5 mL tube and
449 incubated on ice for 30 min. Cells were disrupted by repeated aspiration
450 through a 29-gauge (29G) needle and centrifuged at 20,000 x g 15 min at 4ºC.
451 Pellet was discarded and supernatants, corresponding to total cell lysates, were
452 quantified using the Pierce™ BCA Protein Assay Kit (Thermo Scientific). From
453 total cell lysates, 30 µg were electrophoresed in a 10 % polyacrylamide SDS-
454 PAGE gel, transferred to a nitrocellulose membrane and analyzed by western
455 blot. Rabbit polyclonal anti-GFP-tag (1:500 dilution, # A-11122, Invitrogen) and
456 mouse monoclonal anti-MAL-(E1) (1:500 dilution, # sc-390687, Santa Cruz)
457 followed by secondary polyclonal swine anti-rabbit Immunoglobulins/HRP or
458 polyclonal rabbit anti-mouse Immunoglobulins/HRP respectively (1:2000
459 dilution, #P0217 or #P0161, Dako) were used.
460 The analysis of MAL endogenous protein expression in MOLT-4 cells was
461 performed using a detergent-resistant membranes (DRMs) enrichment protocol.
462 Cells were lysed at 4ºC in 200 µL of lysis buffer containing 1% Triton X-100, 0.5
463 mM EDTA, 1:100 Protease inhibitor cocktail (#P8340, Sigma-Aldrich). Lysates
464 were passed through a 29G needle several times. The insoluble material (Pellet
465 I: nuclei, cytoskeleton, DRMs and unbroken cells) was collected by
466 centrifugation at 20,000 x g for 15 min at 4ºC and the supernatant was
467 discarded. The sediment was resuspended in the lysis buffer supplemented
468 with 60 mM octylglucoside and incubated at 37ºC for 30 min to extract DRMs.
469 The resuspended pellet was centrifuged at 20,000 x g for 15 min at 4ºC. Pellet
470 was discarded and supernatant with the extracted rafts containing MAL was

collected. From total cell lysates, 30 µg were electrophoresed in a 12% polyacrylamide SDS-PAGE gel, transferred to a nitrocellulose membrane and analyzed by western blot. The primary antibodies used were mouse monoclonal anti-MAL-(E1) (1:500 dilution, #sc-390687, Santa Cruz) and mouse monoclonal anti-Flotillin-1, as a loading control (1:1000 dilution, #610821, BD Bioscience). In both cases, the primary antibody was followed by secondary antibody incubation with polyclonal rabbit anti-mouse Immunoglobulins/HRP (1:2000 dilution, #P0161, Dako).

Signal from western blot membranes was developed with Luminata™Crescendo western HRP substrate (Millipore) and detected using an Amersham Imager 600 (GE Healthcare Life Sciences).

**Etx Immunolocalization**

tsA201, RT4-D6P2T and HeLa transfected cells were grown to confluence on coverslips. Cells were washed three times with PBS and fixed with 4% paraformaldehyde (PFA) for 15 min at Room Temperature (RT). After 3 washings with PBS, cells were blocked by adding PBS containing 0.2% gelatin, 20% normal goat serum (NGS) and 0.05% Triton X-100 for 1 h at RT. Next, cells were incubated with 200 nM of Etx labelled with DyLight$^{TM}$ 633 (Etx-633) in PBS containing 0.2% gelatin, 1% NGS, 0.05% Triton X-100 for 1h at RT. After three washes with PBS, coverslips were mounted with Fluoromount aqueous mounting medium (#F4680, Sigma-Aldrich). Etx was labeled with DyLight™ 633 NHS Ester (#46414, Thermo Scientific) following manufacturer's instructions.

Etx immunolocalization on MOLT-4 CTL and MOLT-4 ΔMAL cells was performed starting from 2 x $10^6$ cells. Cells were pelleted at 1,000 x g for 3 min at 4ºC, washed twice with 1 mL PBS and fixed with 500 µL of 4% PFA at RT for 15 min. After fixation, cells were pelleted at 1.000 x g and washed three times with 1 mL PBS containing 1% of Bovine Serum Albumin (PBS-1% BSA). A blocking step with Buffer A (PBS 1X, 0.2% gelatin, 20% Normal Goat Serum (NGS), 3% BSA, 0.05% Triton X-100) was done at RT for 1h followed by an incubation at RT with 500 µL of 100 nM GPF-pEtx in Buffer A for 45 min. After toxin incubation cells were stained with 500 µL of DRAQ5 (1:2000 dilution, #108410, Abcam) in Buffer A for 15 min at RT. Six washing steps were done by centrifugation at 1,000 x g with 1 mL of PBS-1% BSA and 0.05% Triton X-100. Finally, pellet was resuspended with 20 µL of Fluoromount aqueous mounting medium (#F4680, Sigma-Aldrich) and placed on a coverslip.

Samples were analyzed by confocal microscopy in a Leica TCS-SL spectral confocal microscope at CCiTUB, Biology Unit of the Bellvitge Campus, University of Barcelona.

**hMAL-CRISPR-Cas9**

hMAL sgRNAs were designed using the sgRNA Scorer 2.0 CRISPR Design Tool (46). Several sgRNA sequences were obtained. From the list, two hMAL-sgRNA were selected; one matching in the 5'UTR and the other in the CDS, in a common sequence of hMAL mRNA variants.

hMAL-5'UTR-sgRNA: CCCTGCTCTTAACCCGCGCGCGG, and hMAL-CDS-sgRNA: GCCCCCGCAGCGGCGACGGGGGG. (Underlined nucleotides correspond to PAM sequences and were eluded to design oligonucleotides).

Oligonucleotides, including the selected sequences and overhangs for the ligation step into the pair of BbsI, were phosphorylated, annealed and cloned into a pSPCas9(BB)-2A-GFP vector (Adgene plasmid ID:48138) as described in Ran et. al. (47). Both hMALsgRNA constructs: hMAL-5'UTRsgRNA-pSPCAS9(BB)-2A-GFP and hMAL-CDSsgRNA-pSPCAS9(BB)-2A-GFP, were cotransfected into MOLT-4 cells by electroporation to obtain MOLT-4 ΔMAL cells. In parallel an empty pSPCAS9(BB)-2A-GFP vector was also transfected into MOLT-4 cells to obtain a MOLT-4 CRIPSR control cell line, MOLT-4 CTL. Cells were transfected by electroporation using Gene Pulser® with 4 mm gap cuvettes (BioRad), at 300 V, 10 ms, 1 pulse in ECM 830 Electro Square Porator™ (BTX) electroporator.

After 24 h of transfection, a pool of positive GFP cells was selected using the cell sorter MoFlo Astrios (Beckman Coulter) at CCiTUB, Biology Unit of the Bellvitge Campus, University of Barcelona. Afterwards, a clonal selection from the positive GFP pools was done using the same cell sorter. Clones were functionally checked performing cytotoxicity assays.

**Cytotoxicity assays**

The cytotoxic effect of Etx was measured using the MTS (3-(4, 5-dimethylthiazol-2-yl)-5-(3-carboxymethoxyphenyl)-2-(4-sulfophenyl)-2H-tetrazolium) colorimetric assay. Cells were set into 96-well cell culture plate at confluence (tsA201, RT4-D6P2T and HeLa cells) or 80.000 cells/well for lymphoid cell lines in 100 µL RPMI (Gibco) supplemented with 10% FBS (Biological Industries), media. Cells were exposed to increasing concentrations

of Etx (0, 6.25, 12.5, 25, 50 and 100 nM) for 1-2 h at 37ºC. Controls were obtained by omitting Etx in each condition (100% of cell viability) or by adding 0.1% TritonX-100 (100% of cell lethality). After incubation, 20 µL CellTiter 96® $AQ_{ueous}$ One Solution Cell Proliferation Reagent Solution (#G3581, Promega) were added to each well. The amount of formazan product obtained from the reaction, was recorded spectrophotometrically at 490 nm in a Microplate reader, Biochrom® Asys UVM 340 (Biochrom), at CCiTUB, Biology Unit of the Bellvitge Campus, University of Barcelona.

The absorbance obtained was directly proportional to the number of living cells in culture. Triplicates of the assay were performed in three independent experiments for each condition. Statistics were determined by nonlinear regression analysis using a two-way ANOVA followed by Tukey's multiple comparisons test.

$CT_{50}$ values for cytotoxicity tests were determined from MTS assays absorbance values using a nonlinear regression model (curvefit) based on sigmoidal dose response curve, log (inhibitor) versus normalized response. $CT_{50}$ was calculated with a 95% confidence interval indicated as 95% CI (lower-upper).

**Luciferin-luciferase detection assay**

Etx-dependent ATP release from cells was measured using the Luciferin-Luciferase method.

Adherent cells (tsA201, RT4-D6P2T, HeLa) were plated into a black 96 well plate with clear flat bottom and grown into confluence in 100 µL medium, in





Molecular and Cellular Biology

569 case of suspension cells (JeKo-1, TK6, MOLT-4 and Jurkat), 80,000 cells/well
570 were seeded in 100 µL of medium.
571 Luciferase extract lantern from *Photinus pyralis* (Sigma-Aldrich) was
572 resuspended at 0.1 µg/µL and desalted in a 10 mL 10 DG column (Bio-Rad). D-
573 luciferin (Sigma-Aldrich) was diluted at a concentration of 0.7 µg/µL in ultrapure
574 water and was adjusted with NaOH to a final PH 7.4.
575 A mixture of 5 µL of D-luciferin and 5 µL of luciferase were added in each cell
576 well. Light emitted when ATP reacted with luciferin and luciferase was recorded
577 in a FLUOstar OPTIMA Microplate Reader (BMG) at CCiTUB, Biology Unit of
578 the Bellvitge Campus, Universitat Barcelona. Once the basal recording signal
579 was stable, pEtx or Etx were added to each well to obtain the desired final
580 concentration. When the peak of bioluminescence returned to the basal level,
581 Triton X-100 was added to evaluate the content of ATP still present into cells.
582 Each condition was run in triplicates in three independent experiments.
583 Statistics were determined by nonlinear regression analysis using a two-way
584 ANOVA, followed by Sidak's multiple comparisons test.
585

586 **Oligomer complex formation**

587 Etx cytotoxic activity is correlated with the formation of large membrane
588 complexes (20). To observe the formation of Etx complexes in the plasma
589 membrane, cells were grown, and incubated with pEtx and Etx at 100 nM for 30
590 min h at 37ºC. Cells were pelleted by centrifugation at 800 x g, washed once
591 with PBS and centrifuged at 800 x g. Pellets were resuspended with 500 µL of
592 RIPA buffer supplemented with 1:100 Protease inhibitor cocktail (#P8340,
593 Sigma-Aldrich), maintained on ice 30 min and homogenized by passage

through a 29-gauge needle. The lysed cells were centrifuged at 20,000 x g 15 min. Supernatants, corresponding to total cell lysates, were quantified by Pierce™ BCA Protein Assay Kit (Thermo Scientific). 30 µg of total cell lysates and 1 ng of recombinant pEtx and Etx as controls to detect correct band size were electrophoresed in a 10% polyacrylamide SDS-PAGE gel and were transferred to nitrocellulose membranes. Membranes were analyzed by western blot using a rabbit polyclonal anti-pEtx (14) pre-adsorbed to cell extracts (1:500 dilution), followed by polyclonal swine anti-rabbit immunoglobulins/HRP (1:15000 dilution, #P0217, Dako). The same membranes were developed with anti-αTubulin Clone DM 1A (1:2000 dilution, #T9026, Sigma-Aldrich) followed by rabbit anti-mouse Immunoglobulins/HRP (1:15000 dilution, #P0161, Dako) to obtain the loading control. Membranes were developed with Luminata™Crescendo western HRP substrate (Millipore) and signal was detected using an Amersham Imager 600 (GE Healthcare Life Sciences).

**Coimmunoprecipitation**

The association of Etx and MAL was studied by coimmunoprecipitation (co-IP), which allows the study of protein-protein interactions. In Co-IP the complexes containing the target protein are incubated with an antibody, then Sepharose protein A or protein G beads are added to adsorb the antibody-protein complexes which are obtained by centrifugation. Protein components in the complexes are visualized by western blot analysis using specific antibodies raised against the different components.

HeLa-GFP (HeLa-pEGFPN1) and HeLa-MALGFP (HeLa-pEGFPN1-hMAL) cells were grown to confluence in 10 cm diameter cell culture dishes. From four

HeLa-pEGFPN1-hMAL cell culture dishes, one was incubated for 30 min at 37ºC with pEtx at 100 nM, two with Etx at 100 nM, and the fourth was kept as a negative control. Cells were washed once with PBS,. scraped and resuspended with 500 µL of RIPA buffer supplemented with protease inhibitor cocktail (#P8340, Sigma-Aldrich). Cells were collected in a 1.5 mL tube and maintained on ice for 30 min. Suspensions were disrupted by repeated aspiration through a 29-gauge needle. The lysed cells were centrifuged at 20,000 x g for 15 min, and the pellet was discarded. From the cell lysates, 20 µL (4% total volume) of each condition were separated as input samples and 10 µL of 3x protein loading buffer (187.5 mM Tris-HCl pH 6.8, 2% SDS, 0.006% bromophenol blue, and 30% glycerol) containing 1% β-Mercaptoethanol were added to each input.

A pre-clear lysate was obtained by adding 20 µL of Protein G Plus/Protein A Agarose Suspension beads (# IP-05, Merck) to the samples, which were incubated on a rotating device at 4ºC for 1 h. Beads were pelleted by centrifugation at 1,000 x g for 2 min at 4ºC. Supernatants were transferred to a 1.5 mL tube and 2 µg of mouse monoclonal anti-GFP, clone GFP-20 (# G6539 Sigma-Aldrich) were added to all tubes except in one tube, previously incubated with 100 nM Etx, that was incubated with 2 µg of mouse monoclonal anti-αTubulin Clone DM 1A (#T9026, Sigma-Aldrich) as a negative control. Tubes were incubated overnight on a rotating device at 4ºC. A volume of 30 µL of Protein G Plus/Protein A Agarose suspension beads was added to each tube and incubated at 4ºC in a rotating device for 2 h. Immunoprecipitates adsorbed to beads were collected by centrifugation at 1.000 x g for 2 min at 4ºC. Supernatants were carefully aspirated and discarded. Pellets were washed 4 times with 1 mL RIPA buffer, each time repeating the above centrifugation step.

After the final wash, supernatants were aspirated and the resulting pellets were resuspended in 20 µL protein loading buffer containing 1% ß-Mercaptoethanol. All samples, were heated for 5 min at 95 ºC, and centrifuged at 1,000 x g for 2 min at 4 ºC to separate the agarose beads. Inputs, supernatants and recombinant proteins pEtx and Etx were loaded in a 10% polyacrylamide SDS-PAGE gel, transferred to a nitrocellulose membrane and detected by western blot analysis with anti-pEtx rabbit polyclonal antibody pre-adsorbed to cell extracts (1:500 dilution) (14), followed by secondary polyclonal swine anti-rabbit Immunoglobulins/HRP (1:15000 dilution, #P0217, Dako), to reveal the coimmunoprecipitated and Etx.

Afterwards, the same membrane was re-blotted to check the immunoprecipitated MAL-GFP with mouse monoclonal anti-GFP clone GFP-20 (1:500 dilution, # G6539, Sigma-Aldrich) followed by secondary polyclonal rabbit anti-mouse Immunoglobulins/HRP (1:15000 dilution, #P0161, Dako).

Signal from membranes was developed with Luminata™Crescendo western HRP susbtrate (Millipore) and detected using an Amersham Imager 600 (GE Healthcare Life Sciences).

**RT-PCR**

A total RNA extraction was realized in TK6, JeKo-1, MOLT-4 and Jurkat-1 cells using the RNeasy Mini Kit (Qiagen) following manufacturer's instructions.

The concentration of each sample was recorded spectrophotometrically at 260 nm in a Nanodrop2000C spectrophotometer (Thermo Scientific). A retrotranscription reaction (1.5 µg RNA) was carried out by using the RevertAid First Strand cDNA Synthesis Kit (Thermo Scientific) following the protocol

provided by the supplier. PCRs were performed using PCR Master Mix 2x (Thermo Scientific) to detect the presence of hMAL cDNA or 18S rRNA.

hMAL primers:

hMAL Forward, 5'-GCGAAGCTTATGGCCCCCGCAGCGGCGACGGGGGG-3'

and

hMAL Reverse,5'-

GCGCTCGAGTGAAGACTTCCATCTGATTAAAGAGAACACCGC-3'.

18S rRNA primers:

18S Forward: 5'-CGCAGAATTCCCACTCCCGACCC-3' and 18S Reverse: 5'-

CCCAAGCTCCAACTACGAGC-3'.

The reactions were carried out using the following parameters: 95ºC for 2 min, 40 cycles of 95ºC 20 s, 62ºC 10 s and 70ºC for 10 s. Amplicons were detected in a 2 % agarose gel electrophoresis.

**Flow Cytometry**

The flow cytometry experiments to analyze the sensitivity of cells to Etx were performed starting with 6 x $10^6$ cells/ tube. Cells were incubated with 100 nM of Etx-633 in RPMI medium supplemented with 10% FBS for 20 min. Cells were centrifuged at 1.500 x g for 5 min at 4ºC and washed with 1mL PBS-1% BSA, twice. Finally, 5µL of 7AAD (7-Aminoactinomycin) (Invitrogen) were added before flow cytometry analysis. Triplicates of the assay were performed in three independent experiments and statistics were determined by nonlinear regression analysis using a two-way ANOVA followed by Dunnett's multiple comparisons test.

693 To check the binding of Etx to different cell lines cells were incubated during 20
694 min with 100 nM of Etx-633 in RPMI medium supplemented with 10% FBS and
695 3% BSA, centrifuged at 1.500 x g for 5 min at 4ºC and washed with 1mL PBS
696 1% BSA, twice. Cells were fixed with 4% PFA for 15 min at RT. After fixation,
697 cells were pelleted at 1.500 x g and washed three times with 1 mL of PBS-1%
698 BSA. A blocking step with Buffer A (PBS 1X, 0.2% gelatin, 20% Normal Goat
699 Serum (NGS), 3% BSA, 0.05% Triton X-100) was done for 30 min at RT
700 followed by an incubation with mouse monoclonal anti-MAL 6D9 antibody
701 (1:300 dilution) (48) for 30 min at RT in 500 µL of Buffer A. After three washes,
702 cells were centrifuged at 1500 x g and the pellet was resuspended with PBS-1%
703 BSA. Secondary antibody incubation was performed with goat anti-mouse Alexa
704 488 (1:2000 dilution, #A11029, Invitrogen) in Buffer A. Finally, cells were
705 washed three times with PBS-1% BSA. Samples were analyzed in BD FACS
706 Canto (BD Biosciences, San Diego/California, United States) at the Biology Unit
707 of the Bellvitge Campus, University of Barcelona and data was analysed using
708 the FlowJo software (FlowJo LLC, Ashland, Oregon, United States).
709
710 **Quantification and Statistical Analysis**
711 Statistical parameters, including assays, n values, comparison tests and
712 statistical significance are reported in the detailed methods section, Figures and
713 Figure Legends. In Figures, asterisks denote statistical significance as
714 calculated by nonlinear regression analysis using a two-way ANOVA test and
715 each p value is indicated in Figure Legends.
716 All statistics were analyzed using GraphPad Prism version 7.00 for Windows,
717 GraphPad Software, La Jolla, California, USA.

## ACKNOWLEDGMENTS

The authors thank Inmaculada Gómez de Aranda, the CCiTUB Biology Unit of the Campus de Bellvitge for their technical assistance, Dr. Miguel Angel Alonso from the Centro de Biología Molecular Severo Ochoa (CSIC-UAM, Spain), for anti-MAL 6D9 antibody and useful comments, Dr. Joan Gil from the Department of Physiological Sciences of the University of Barcelona for the TK6, Jurkat and JeKo-1 cell lines and Dr. Mireia Martin from the Pathology and Experimental Therapeutics Department of the University of Barcelona for the 18S rRNA primers. This work was supported by grants SAF2014-56811-R and SAF2017-85818-R from Ministerio de Economía, Industria y Competitividad, la Agencia Estatal de Investigación y el Fondo Europeo de Desarrollo Regional (FEDER) to JB and CS.


## REFERENCES


1. Payne D, Oyston P. 1997. The *Clostridium perfringens* epsilon toxin. Academic Press, San Diego.
2. Songer JG. 1996. Clostridial enteric diseases of domestic animals. Clin Microbiol Rev 9:216-234.
3. Uzal FA, Songer JG. 2008. Diagnosis of Clostridium perfringens intestinal infections in sheep and goats. J Vet Diagn Invest 20:253-265.
4. Minami J, Katayama S, Matsushita O, Matsushita C, Okabe A. 1997. Lambda-toxin of Clostridium perfringens activates the precursor of

epsilon-toxin by releasing its N- and C-terminal peptides. Microbiol Immunol 41:527-535.

5. Miyamoto O, Minami J, Toyoshima T, Nakamura T, Masada T, Nagao S, Negi T, Itano T, Okabe A. 1998. Neurotoxicity of Clostridium perfringens epsilon-toxin for the rat hippocampus via the glutamatergic system. Infect Immun 66:2501-2508.

6. Cole AR, Gibert M, Popoff M, Moss DS, Titball RW, Basak AK. 2004. Clostridium perfringens epsilon-toxin shows structural similarity to the pore-forming toxin aerolysin. Nat Struct Mol Biol 11:797-798.

7. Popoff MR. 2014. Clostridial pore-forming toxins: powerful virulence factors. Anaerobe 30:220-238.

8. Popoff M. 2011. Epsilon toxin: a fascinating pore-forming toxin. FEBS J 278:4602-4615.

9. Dorca-Arevalo J, Soler-Jover A, Gibert M, Popoff M, Martin-Satue M, Blasi J. 2008. Binding of epsilon-toxin from Clostridium perfringens in the nervous system. Vet Microbiol 131:14-25.

10. Wioland L, Dupont J, Doussau F, Gaillard S, Heid F, Isope P, Pauillac S, Popoff M, Bossu J, Poulain B. 2015. Epsilon toxin from Clostridium perfringens acts on oligodendrocytes without forming pores, and causes demyelination. Cell Microbiol 17:369-388.

11. Linden J, Ma Y, Zhao B, Harris J, Rumah K, Schaeren-Wiemers N, Vartanian T. 2015. Clostridium perfringens Epsilon Toxin Causes Selective Death of Mature Oligodendrocytes and Central Nervous System Demyelination. Mbio 6:e02513.

12. Rumah KR, Linden J, Fischetti VA, Vartanian T. 2013. Isolation of Clostridium perfringens type B in an individual at first clinical presentation of multiple sclerosis provides clues for environmental triggers of the disease. PLoS One 8:e76359.

13. Tamai E, Ishida T, Miyata S, Matsushita O, Suda H, Kobayashi S, Sonobe H, Okabe A. 2003. Accumulation of Clostridium perfringens epsilon-toxin in the mouse kidney and its possible biological significance. Infect Immun 71:5371-5375.

14. Soler-Jover A, Blasi J, Gómez de Aranda I, Navarro P, Gibert M, Popoff MR, Martín-Satué M. 2004. Effect of epsilon toxin-GFP on MDCK cells and renal tubules in vivo. J Histochem Cytochem 52:931-942.

15. Chassin C, Bens M, de Barry J, Courjaret R, Bossu JL, Cluzeaud F, Ben Mkaddem S, Gibert M, Poulain B, Popoff MR, Vandewalle A. 2007. Pore-forming epsilon toxin causes membrane permeabilization and rapid ATP depletion-mediated cell death in renal collecting duct cells. Am J Physiol Renal Physiol 293:F927-937.

16. Shortt SJ, Titball RW, Lindsay CD. 2000. An assessment of the in vitro toxicology of Clostridium perfringens type D epsilon-toxin in human and animal cells. Hum Exp Toxicol 19:108-116.

17. Fernandez Miyakawa ME, Zabal O, Silberstein C. 2011. Clostridium perfringens epsilon toxin is cytotoxic for human renal tubular epithelial cells. Hum Exp Toxicol 30:275-282.

18. Ivie SE, Fennessey CM, Sheng J, Rubin DH, McClain MS. 2011. Gene-trap mutagenesis identifies mammalian genes contributing to

intoxication by Clostridium perfringens epsilon-toxin. PLoS One 6:e17787.

19. Gil C, Dorca-Arevalo J, Blasi J. 2015. Clostridium Perfringens Epsilon Toxin Binds to Membrane Lipids and Its Cytotoxic Action Depends on Sulfatide. Plos One 10:e0140321

20. Petit L, Gibert M, Gillet D, Laurent-Winter C, Boquet P, Popoff MR. 1997. Clostridium perfringens epsilon-toxin acts on MDCK cells by forming a large membrane complex. J Bacteriol 179:6480-6487.

21. Nagahama M, Hara H, Fernandez-Miyakawa M, Itohayashi Y, Sakurai J. 2006. Oligomerization of Clostridium perfringens epsilon-toxin is dependent upon membrane fluidity in liposomes. Biochemistry 45:296-302.

22. Rumah K, Ma Y, Linden J, Oo M, Anrather J, Schaeren-Wiemers N, Alonso M, Fischetti V, McClain M, Vartanian T. 2015. The Myelin and Lymphocyte Protein MAL Is Required for Binding and Activity of Clostridium perfringens epsilon-Toxin. Plos Pathogens 11:e1004896.

23. Khalili S, Jahangiri A, Hashemi Z, Khalesi B, Mard-Soltani M, Amani J. 2017. Structural pierce into molecular mechanism underlying Clostridium perfringens Epsilon toxin function. Toxicon 127:90-99.

24. Alonso M, Weissman S. 1987. cDNA clonning and sequence of MAL, a hydrophobic protein associated with human T-cell differentiation. Proc Natl Acad Sci USA 84:1997-2001.

25. Cheong K, Zacchetti D, Schneeberger E, Simons K. 1999. VIP17/MAL, a lipid raft-associated protein, is involved in apical transport in MDCK cells. Proc Natl Acad Sci USA 96:6241-6248.

816 26. Marazuela M, Alonso M. 2004. Expression of MAL and MAL2, two
817 elements of the protein machinery for raft-mediated transport, in normal
818 and neoplastic human tissue. Histol Histopathol 19:925-933.
819 27. Alonso M, Millan J. 2001. The role of lipid rafts in signalling and
820 membrane trafficking in T lymphocytes. J Cell Sci 114:3957-3965.
821 28. Ventimiglia L, Fernandez-Martin L, Martinez-Alonso E, Anton O, Guerra
822 M, Martinz-Menarguez J, Andres G, Alonso M. 2015. Cutting Edge:
823 Regulation of Exosome Secretion by the Integral MAL Protein in T Cells.
824 J Immunol 195:810-814.
825 29. Petit L, Maier E, Gibert M, Popoff MR, Benz R. 2001. Clostridium
826 perfringens epsilon toxin induces a rapid change of cell membrane
827 permeability to ions and forms channels in artificial lipid bilayers. J Biol
828 Chem 276:15736-15740.
829 30. Nestorovich E, Karginov V, Bezrukov S. 2010. Polymer Partitioning and
830 Ion Selectivity Suggest Asymmetrical Shape for the Membrane Pore
831 Formed by Epsilon Toxin. Biophys J 99:782-789.
832 31. Finnie JW. 2004. Neurological disorders produced by Clostridium
833 perfringens type D epsilon toxin. Anaerobe 10:145-150.
834 32. Uzal F, Kelly W, Morris W, Assis R. 2002. Effects of intravenous
835 injection of Clostridium perfringens type D epsilon toxin in calves. J
836 Comp Pathol 126:71-75.
837 33. Finnie JW, Blumbergs PC, Manavis J. 1999. Neuronal damage
838 produced in rat brains by Clostridium perfringens type D epsilon toxin. J
839 Comp Pathol 120:415-420.

840 34. Miyamoto O, Sumitani K, Nakamura T, Yamagami S, Miyata S, Itano T,
841 Negi T, Okabe A. 2000. Clostridium perfringens epsilon toxin causes
842 excessive release of glutamate in the mouse hippocampus. FEMS
843 Microbiol Lett 189:109-113.
844 35. Lonchamp E, Dupont JL, Wioland L, Courjaret R, Mbebi-Liegeois C,
845 Jover E, Doussau F, Popoff MR, Bossu JL, de Barry J, Poulain B. 2010.
846 Clostridium perfringens epsilon toxin targets granule cells in the mouse
847 cerebellum and stimulates glutamate release. PLoS One 5:e13046.
848 36. Uzal F, Vidal J, McClane B, Gurjar A. 2010. *Clostridium Perfringens*
849 Toxins Involved in Mammalian Veterinary Diseases. Open Toxinology J
850 2:24-42..
851 37. Bischofberger M, Iacovache I, van der Goot F. 2012. Pathogenic Pore-
852 Forming Proteins: Function and Host Response. Cell Host Microbe
853 12:266-275.
854 38. Matute C. 2011. Glutamate and ATP signalling in white matter
855 pathology. J Anat 219:53-64.
856 39. Frank M. 2000. MAL, a proteolipid in glycosphingolipid enriched
857 domains: functional implications in myelin and beyond. Prog Neurobiol
858 60:531-544.
859 40. Kim T, Fiedler K, Madison D, Krueger W, Pfeiffer S. 1995. Cloning and
860 characterization of MVP17. A developmentally regulated myelin protein
861 in oligodendrocytes. J Neurosci Res 42:413-422.
862 41. Soler-Jover A, Dorca J, Popoff MR, Gibert M, Saura J, Tusell JM,
863 Serratosa J, Blasi J, Martin-Satue M. 2007. Distribution of Clostridium

perfringens epsilon toxin in the brains of acutely intoxicated mice and its effect upon glial cells. Toxicon 50:530-540.

42. Berer K, Gerdes L, Cekanaviciute E, Jia X, Xiao L, Xia Z, Liu C, Klotz L, Stauffer U, Baranzini S, Kumpfel T, Hohlfeld R, Krishnamoorthy G, Wekerle H. 2017. Gut microbiota from multiple sclerosis patients enables spontaneous autoimmune encephalomyelitis in mice. Proc Natl Acad Sci USA 114:10719-10724.

43. Constantinescu C, Farooqi N, O'Brien K, Gran B. 2011. Experimental autoimmune encephalomyelitis (EAE) as a model for multiple sclerosis (MS). Br J Pharmacol 164:1079-1106.

44. Sonar S, Lal G. 2017. Differentiation and Transmigration of CD4 T Cells in Neuroinflammation and Autoimmunity. Front Immunol 8:1695.

45 Lindner M, Klotz L, Wiendl H. 2018. Mechanisms underlying lesion development and lesion distribution in CNS autoimmunity. J Neurochem doi:10.1111/jnc.14339

46. Chari R, Yeo N, Chavez A, Church G. 2017. sgRNA Scorer 2.0: A Species-Independent Model To Predict CRISPR/Cas9 Activity. ACS Synth Biol 6:902-904.

47. Ran F, Hsu P, Wright J, Agarwala V, Scott D, Zhang F. 2013. Genome engineering using the CRISPR-Cas9 system. Nat Protoc 8:2281-2308.

48. Martin-Belmonte F, Kremer L, Albar J, Marazuela M, Alonso M. 1998. Expression of the MAL gene in the thyroid: the MAL proteolipid, a component of glycolipid-enriched membranes, is apically distributed in thyroid follicles. Endocrinology 139:2077-2084.

889 **FIGURE LEGENDS**

890

891 **Figure 1. Specific binding of Etx to the plasma membrane of hMAL-GFP**
892 **expressing cells lines.**

893 **(A, B)** Western blot analysis of stable tsA201, RT4-D6P2T and HeLa cell lines
894 expressing either GFP or hMAL-GFP. **(A)** Expression of GFP (27kDa, arrow)
895 and hMAL-GFP (44 kDa, arrowhead) was detected with anti-GFP **(B)**
896 Expression of hMAL-GFP (44 kDa, arrowhead) detected with anti-MAL-(E1). **(C)**
897 Confocal microscopy images from tsA201, RT4-D6P2T and HeLa cells
898 expressing hMAL-GFP or GFP and incubated with 100 nM of labeled Etx-633,
899 for 1 hour, see methods. The hMAL-GFP protein (green) exquisitely colocalized
900 with Etx-633 (red) on the plasma membrane while the Etx-633 signal was not
901 detected in control cells, which only express GFP. Scale bar corresponds to 25
902 µm.

903

904 **Figure 2. Etx-dependent ATP release from MDCK cells and from cell lines**
905 **tsA201, RT4-D6P2T and HeLa- expressing hMAL-GFP.**

906 **(A)** ATP release from MDCK cells. MDCK cells were incubated with different
907 concentrations of Etx (arrow indicates Etx addition); the release of ATP was
908 monitored continuously as light emission (A.U. arbitrary Units of luminescence).
909 Etx produced the release of ATP from treated cells at all concentrations used,
910 although kinetics was accelerated at higher Etx concentrations. No ATP release
911 was recorded when MDCK cells were incubated with pEtx at a concentration
912 equivalent to the maximum of the Etx used or when Etx was not added to the
913 incubation medium (0 nM). Insert: at the end of experiment, Triton X-100 was

added (0.2% final concentration, arrowhead) to release the remaining ATP. The release of the ATP content was clearly observed in control cells (0 mM) and when cells were incubated with pEtx. **(B-D)** ATP release from hMAL-GFP or GFP expressing cells: tsA201 cells (B), RT4-D6P2T cells (C) and HeLa cells (D). Etx (100 nM) was added (arrow) to transfected cell lines expressing hMAL-GFP or GFP alone and ATP release was monitored as in **(A)**. ATP was released only from cells expressing hMAL-GFP protein (black line) but not from cells expressing GFP alone (grey line). Triton X-100 (0.2 % final concentration) was added at the end of the experiment to estimate the total content of ATP in cells (not shown). **(E)** Bar chart shows the percentage of the Etx-induced release of ATP with respect to the total ATP content in each condition **(B-D)**. Each condition was run in triplicates and in three independent experiments (****$p<0.0001$).

**Figure 3. Cytotoxic effect of Etx on hMAL expressing cells (tsA201, RT4-D6P2T and HeLa).**

MTS assay was performed to determine cell viability after incubating the cells with increasing concentrations of Etx for 1 hour. Results from three independent experiments were represented as percentage of cell survival along different Etx concentration. The cytotoxicity of Etx on hMAL-GFP expressing cells was dose dependent as on MDCK cells, while no effect was observed on control cells expressing GFP alone. Each condition was run in triplicates and in three independent experiments (****$p<0.0001$, for clarity, only hMAL-GFP expressing cells were labeled with asterisk).

939 **Figure 4. Immunoprecipitation assays reveal a direct interaction between**
940 **hMAL and Etx.**
941 Coimmunoprecipitation of Etx by anti-GFP antibody in hMAL-GFP HeLa stable
942 cell line. Cells were treated or not with 100 nM of pEtx or Etx, for 30 minutes.
943 Immunoprecipitation of hMAL-GFP was performed with anti-GFP antibody (α-
944 GFP); anti-αTubulin antibody (α-Tub) was used as a negative control. Upper
945 pannel: western blotting revealed with anti-pEtx antibody. On the left, inputs
946 from cell lysates revealed pEtx and Etx monomers (33 kDa black arrow, and 29
947 kDa black arrowhead, respectively) and Etx protein complexes (>250 kDa, grey
948 arrowhead). On the centre, immunoprecipitated samples (IP) with α-GFP or α-
949 Tub, as a negative control. Results showed the coimmunoprecipitation of Etx
950 complexes (>250 kDa grey arrowhead) from α-GFP IP, but no signal was
951 detected from α-Tub IP. On the right: pEtx and Etx recombinant proteins.
952 Asterisk indicates a non-specific band present in all lanes. Lower pannel:
953 western blot analysis from the same membrane analyzed with α-GFP. hMAL-
954 GFP was detected as a band of 44 kDa. Notice that α-Tub IP do not
955 immunoprecipitate hMAL-GFP. This is a representative example from a
956 threefold repeated experiment.
957
958 **Figure 5. Lymphocytic cell lines expressing MAL are sensitive to Etx.**
959 **(A)** RT-PCR detection of endogenous hMAL mRNA on MOLT-4 and Jurkat,
960 lymphocytic T cell lines, but not on TK6 and JeKo-1 cell lines. The18S rRNA
961 was used as control. **(B)** MTS assay was performed, as in figure 3, to determine
962 cell viability after treatment of cells (JeKo-1, TK6, MOLT-4 and Jurkat) with
963 increasing concentrations of Etx for 1 hour. The cytotoxicity of Etx on MOLT-4

964 and Jurkat cells was dose dependent, while no effect was observed on TK6 and
965 JeKo-1 lymphocytic B cell lines. Triplicates of three independent experiments
966 were represented as percentage of cell survival along different Etx
967 concentrations. (****p<0.0001). **(C)** Percentage of ATP released from JeKo-1,
968 TK6, MOLT-4 and Jurkat cells after the treatment with 100nM of pEtx or Etx.
969 MOLT-4 cells and Jurkat cells were sensitive to Etx, being the ATP release
970 highest in MOLT-4 cells, whereas no ATP release was observed in JeKo-1 and
971 TK6 lymphocitic B cell lines. Notice that no ATP release was detected when
972 cells were incubated with pEtx at the maximum concentration used with Etx
973 (100 nM). The histograms were obtained from triplicates of three independent
974 experiments (****p<0.0001).
975
976 **Figure 6**. **Etx cytotoxicity on MOLT-4 and Jurkat Lymphocytic T cell lines**
977 **is the result of oligomerization.**
978 **(A)** Flow cytometry and cell viability of JeKo-1, MOLT-4 and Jurkat cell lines
979 after Etx incubation. Cells were incubated with 0, 10 and 100 nM of pEtx or Etx
980 for 20 minutes and analyzed after 7AAD staining. Histogram analysis of 7AAD
981 signal revealed that MOLT-4 and Jurkat cells were sensitive to Etx while Jeko-1
982 cells were not sensitive at all (bar indicates death cells stained with 7AAD).
983 Note that as in the case of Jeko-1, no cells were dying after pEtx incubation.
984 (Represented results from one of three independent experiments). **(B)** Bar chart
985 of cell death percentage from flow cytometry assays explained above. Results
986 were obtained from three independent experiments (** p=0.0058, ****p=0.0001).
987 **(C)** JeKo-1 and MOLT-4 cell lines were treated with 100 nM of pEtx or Etx for
988 30 min. Western blot analysis of cell lysates using anti-pEtx revealed high

molecular weight complexes (>250 kDa, black arrowhead) and monomeric forms of pEtx (33 kDa, black arrow) in MOLT-4 cells, but very low levels or no detection of pEtx or Etx was observed in JeKo-1 cell line. . Recombinant pEtx and Etx were used as controls in the gels to define the correct size bands and membrane was developed with anti-αTubulin to obtain a loading control signal. The experiment was repeated three times.

**Figure 7. Etx binding depends on MAL expression.**

**(A)** Western blot analysis of MOLT-4 CTL and MOLT4-ΔMAL with anti-MAL (E1) antibody and anti-Flotillin-1 antibody, as a loading control. After applying Crisp-Cas9 technology, MAL protein was absent on MOLT4-ΔMAL cells (upper panel). . The experiment was repeated tree times. **(B)** Confocal microscopy images from MOLT-4 CTL and MOLT4-ΔMAL pelleted cells incubated previously with 100 nM pEtx-GFP for 45 min. Nuclei were stained with DRAQ5 (blue). The high density of cells is the result to observe pelleted cells resuspended in 20 µl and placed as a drop on a coverslip. Intense fluorescent signal due to the pEtx binding was observed on the plasma membrane of MOLT-4 CTL cells (green) but not on MOLT4-ΔMAL cells. Scale bar corresponds to 5 µm. **(C)** Flow cytometry analyses revealed the absence of Etx binding on MOLT-4 ΔMAL cells compared to MOLT-4 CTL after incubation of cells with Etx-633 100 nM for 20 min. **(D)** Flow cytometry analyses after incubation with anti-MAL 6D9 followed by Alexa 488 secondary antibody showed no anti-MAL 6D9 binding on MOLT-4 ΔMAL cells. Notice that MOLT-4 ΔMAL revealed no Etx binding nor anti-MAL 6D9 binding due to the absence of MAL protein, as happens in JeKo-1 control cells.

**Figure 8. Neither the cytotoxicity nor the Etx binding and their oligomeric complexes are detected on MOLT-4 ΔMAL cells.**

**(A)** MTS assay performed to determine cell viability after incubation of cells with increasing concentrations of Etx for 1 h. The cytotoxicity of Etx on MOLT-4 and MOLT-4 CTL cells was dose dependent, while no effect was observed on MOLT-4 ΔMAL cells. Results represented the percentage of cell survival from three independent experiments. (****p<0.0001). **(B)** MOLT-4 CTL and MOLT-4 ΔMAL cells were treated with 100 nM of pEtx or Etx for 30 min. Western blot analysis of cell lysates using anti-pEtx revealed oligomeric complexes (> 250 kDa, black arrowhead) and also monomeric forms of pEtx (33 kDa, black arrow) and Etx (29 kDa, grey arrow) in MOLT-4 CTL. No pEtx or Etx nor oligomeric complexes were oberved in MOLT-4 ΔMAL cells. Recombinant pEtx and Etx were used as controls in the gels to define the correct size bands and membrane was developed with anti-αTubulin to obtain a loading control signal. The experiment was repeated three times.

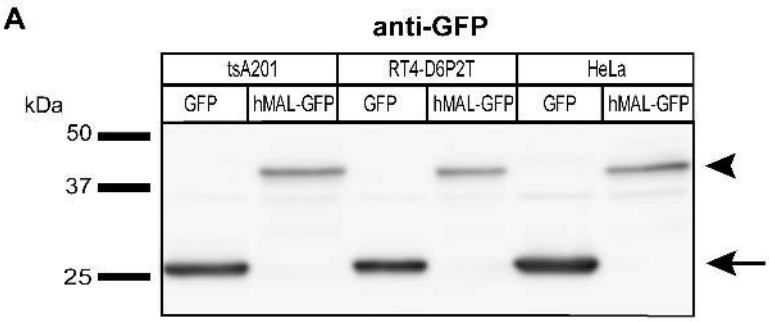


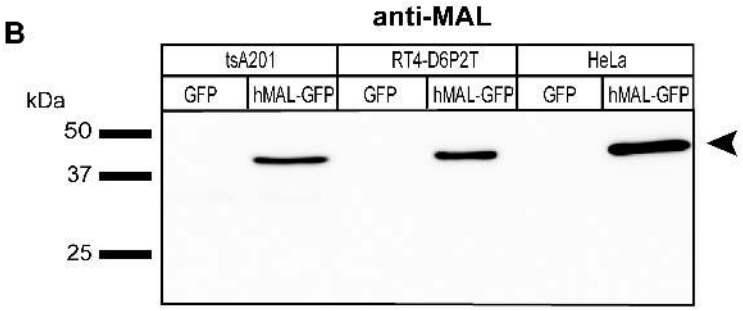


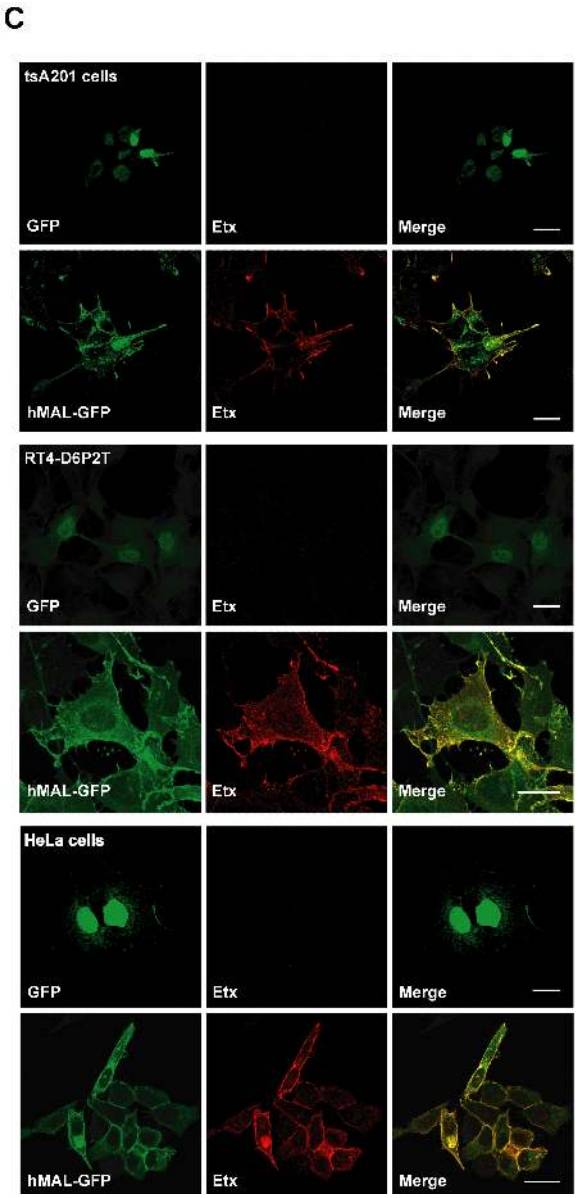

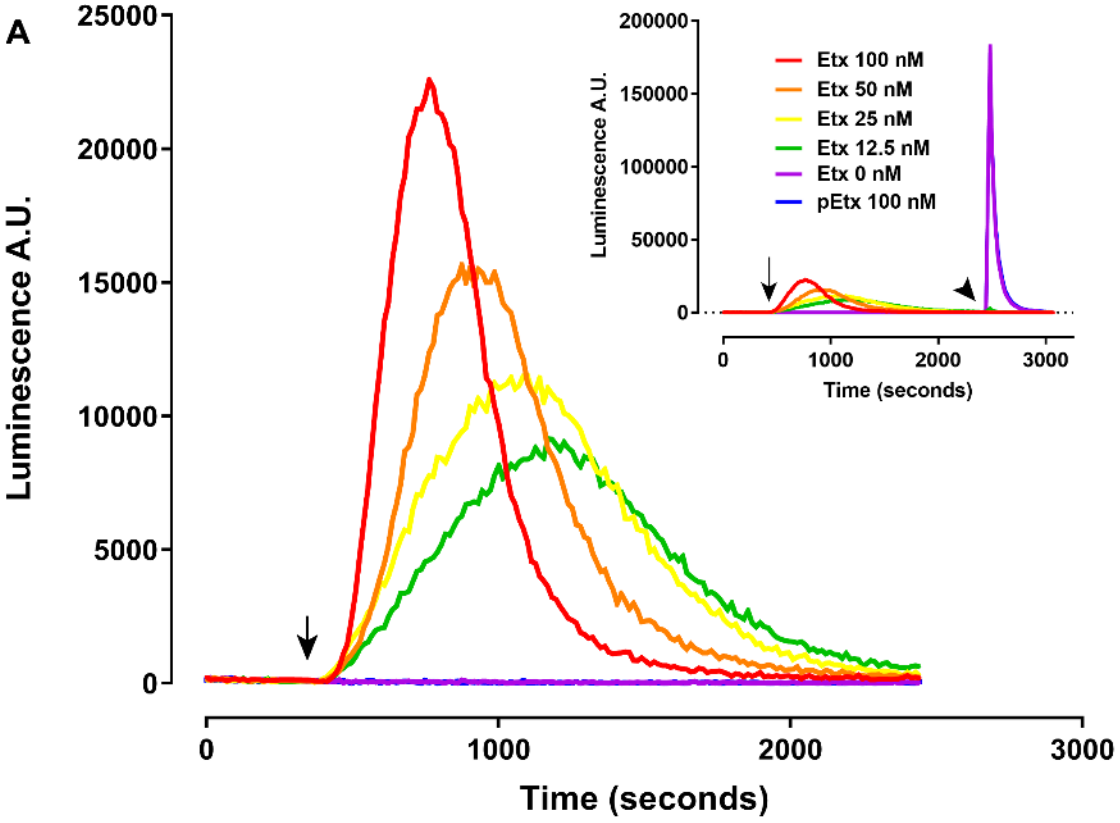


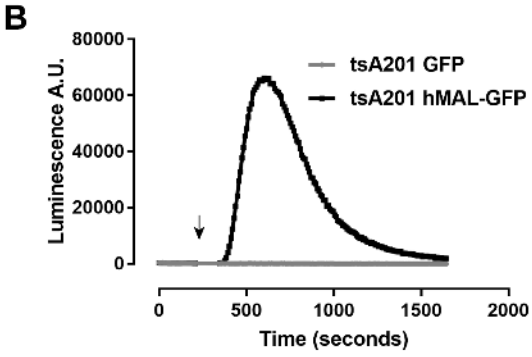


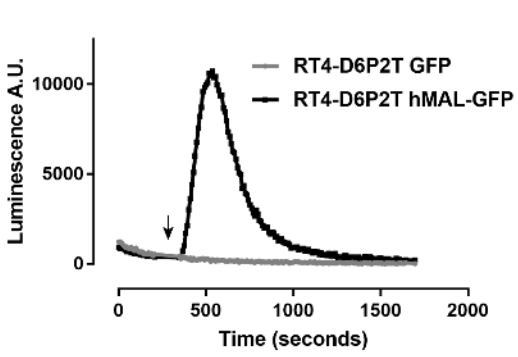


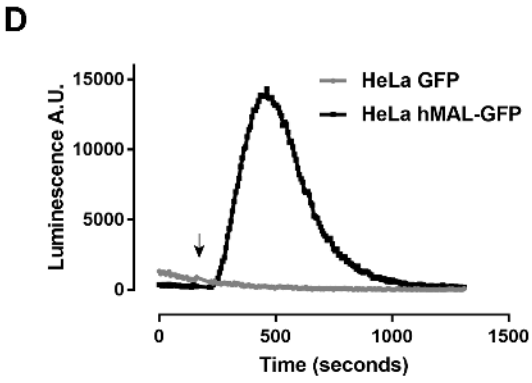


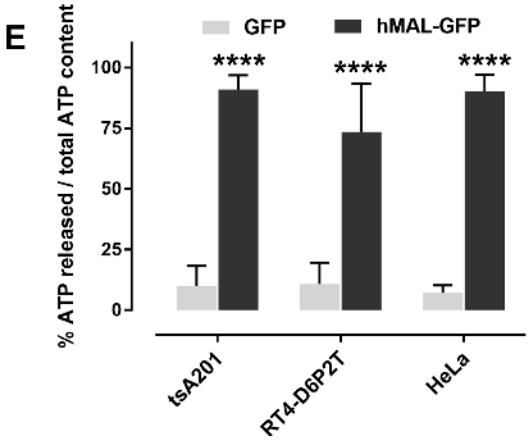

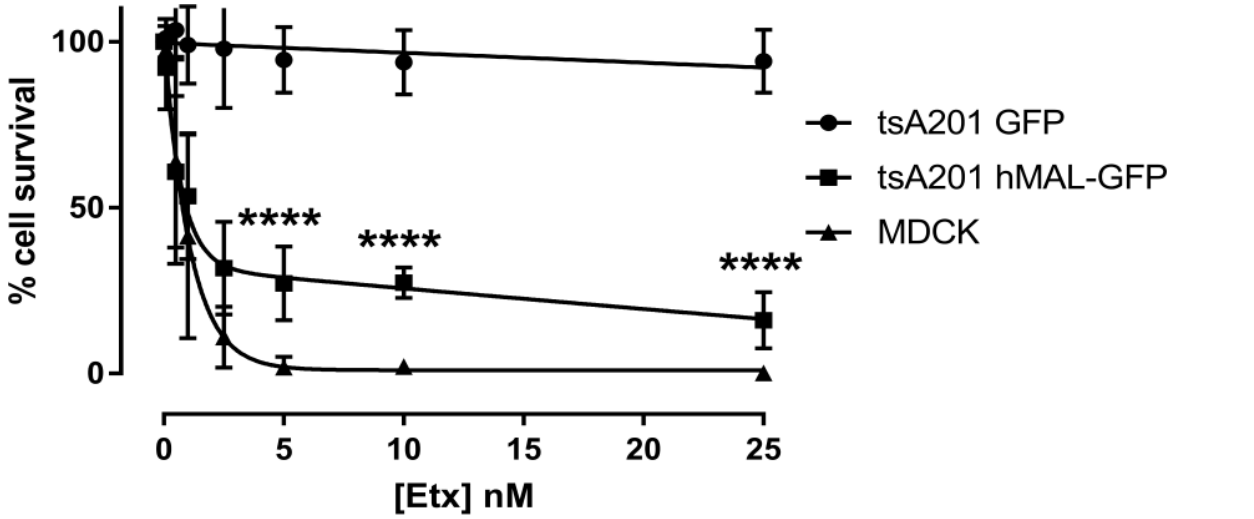


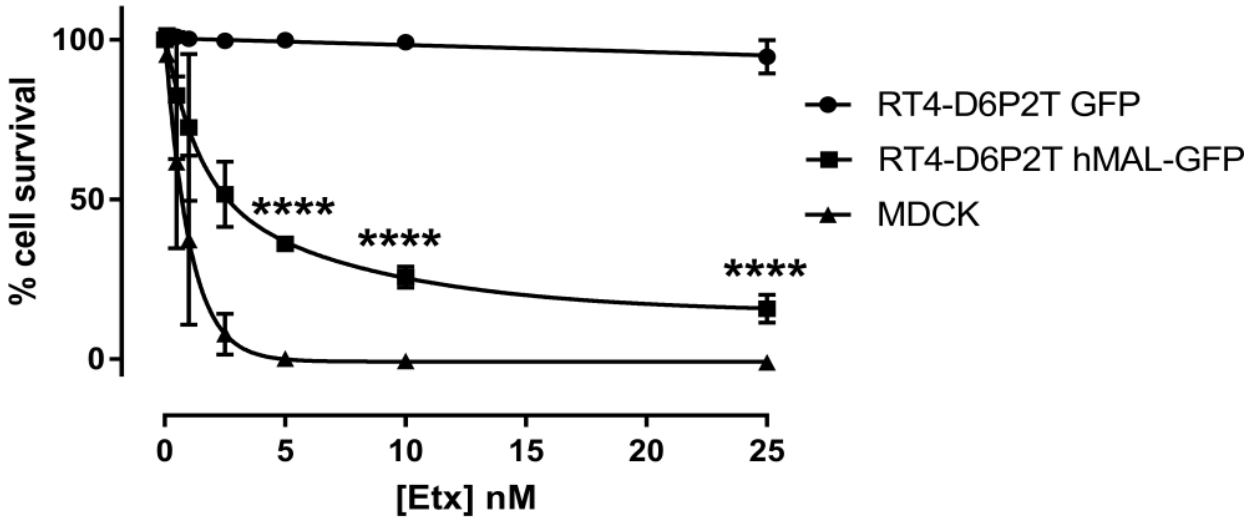


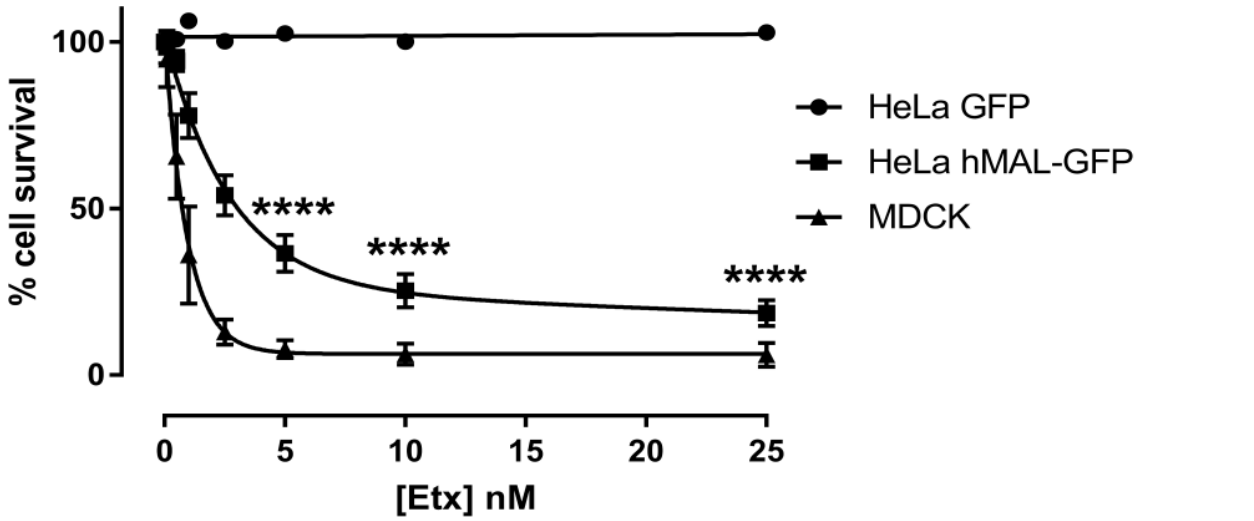

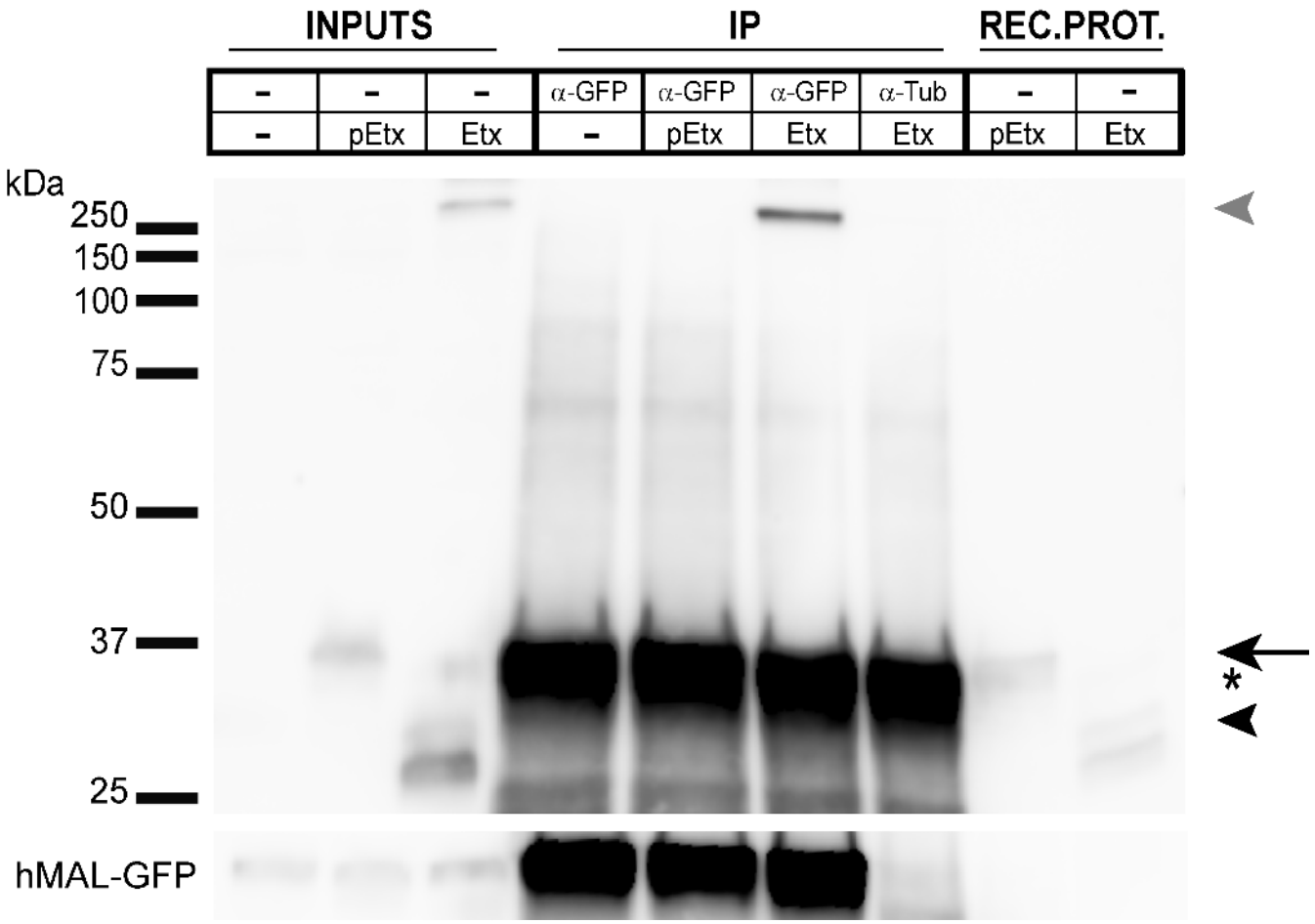

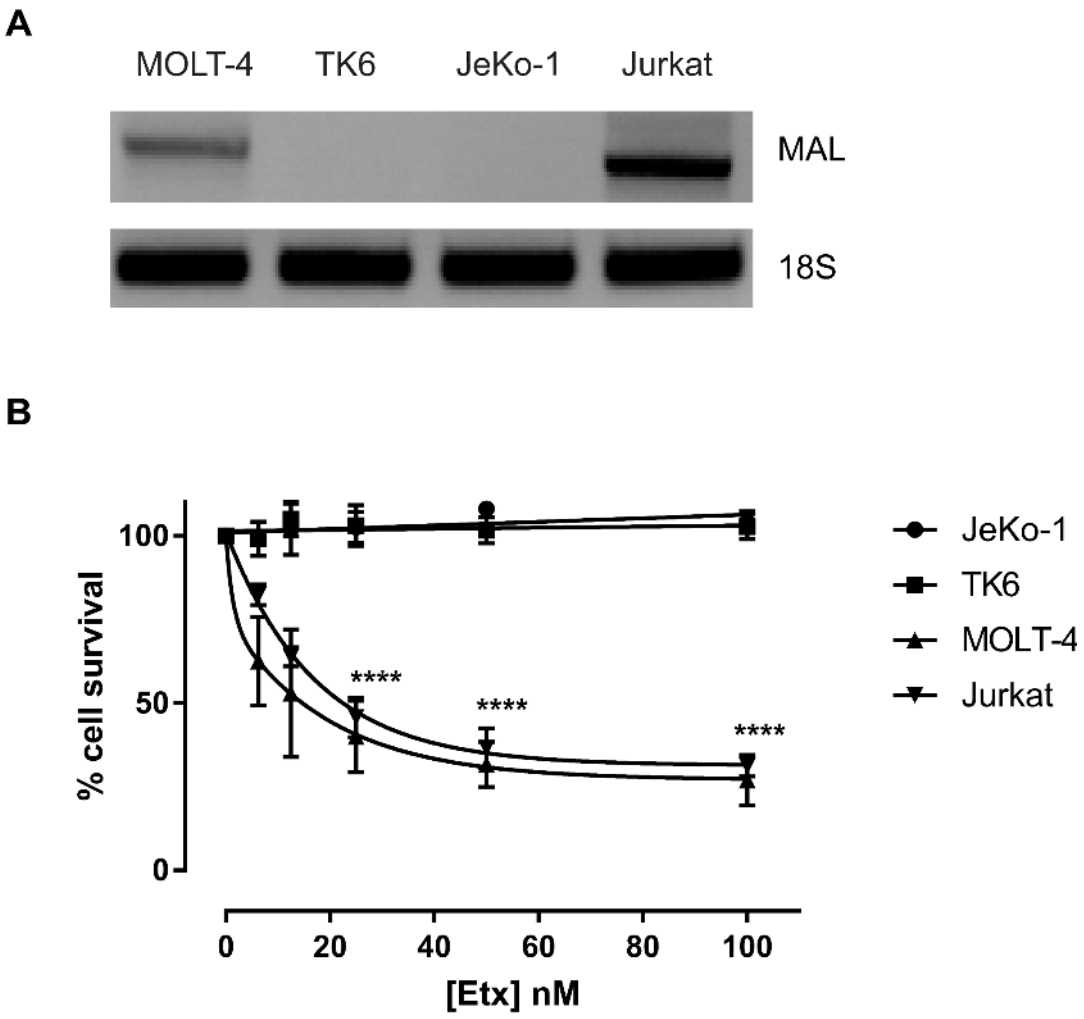

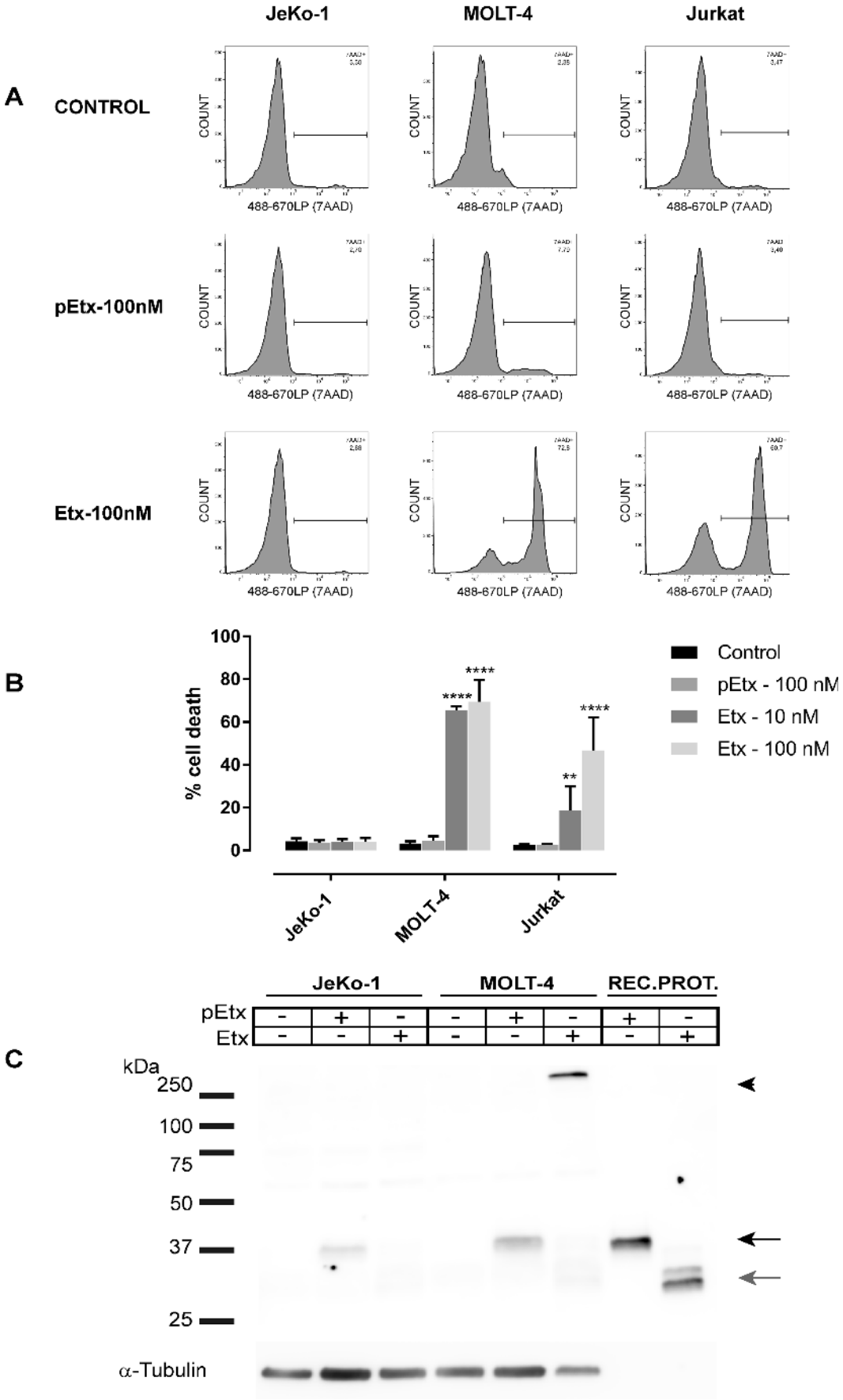

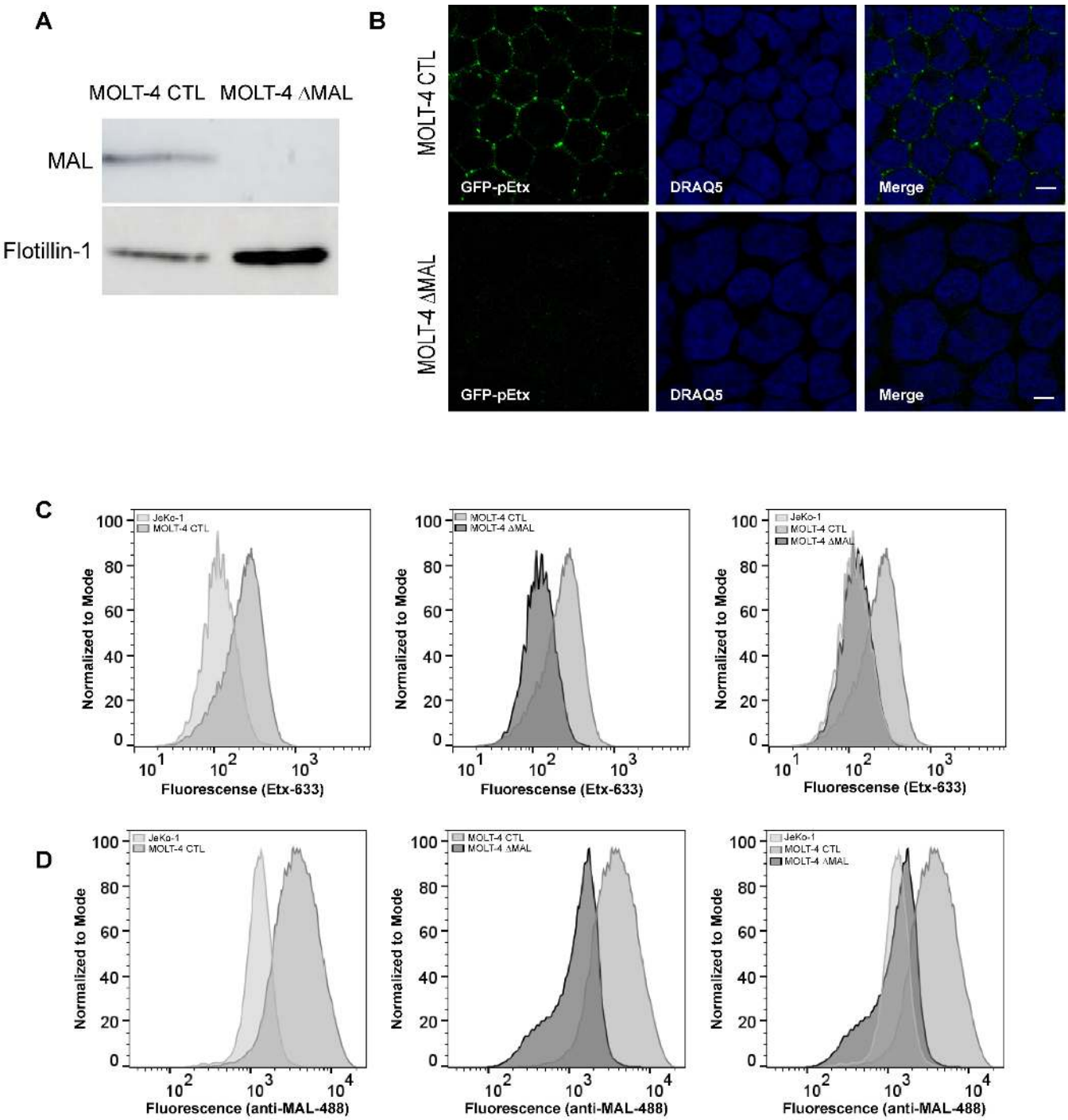

A

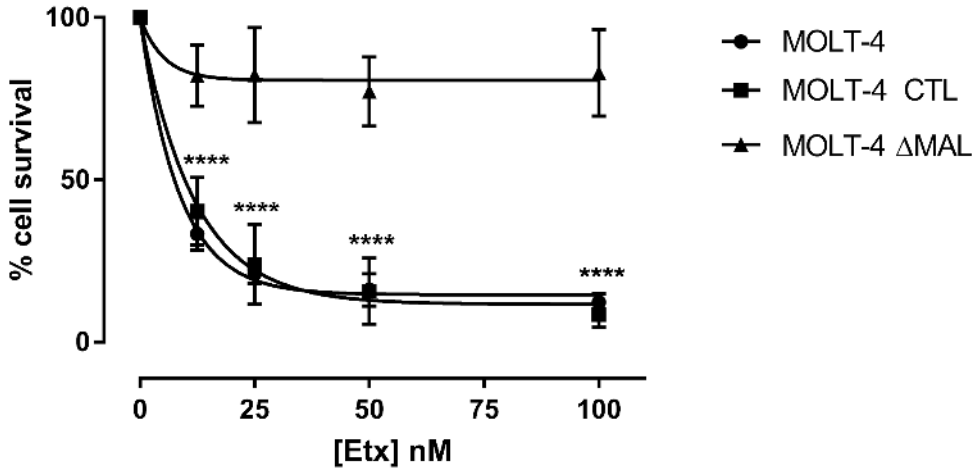


B